



Contents lists available at ScienceDirect

# Journal of Sound and Vibration

journal homepage: [www.elsevier.com/locate/jsvi](http://www.elsevier.com/locate/jsvi)

## Approximation of the Duffing oscillator frequency response function using the FPK equation

E.J. Cross, K. Worden\*

Dynamics Research Group, Department of Mechanical Engineering, University of Sheffield, Mappin St, Sheffield S1 3JD, UK

### ARTICLE INFO

#### Article history:

Received 17 October 2009

Received in revised form

23 August 2010

Accepted 24 August 2010

Handling Editor: L.N. Virgin

Available online 29 September 2010

### ABSTRACT

Although a great deal of work has been carried out on nonlinear structural dynamic systems under random excitation, there has been a comparatively small amount of this work concentrating on the calculation of the quantities commonly measured in structural dynamic tests. Perhaps the most fundamental of these quantities is the frequency response function (FRF). A number of years ago, Yar and Hammond took an interesting approach to estimating the FRF of a Duffing oscillator system which was based on an approximate solution of the Fokker–Planck–Kolmogorov equation. Despite reproducing the general features of the statistical linearisation estimate, the approximation failed to show the presence of the poles at odd multiples of the primary resonance which are known to occur experimentally. The current paper simply extends the work of Yar and Hammond to a higher-order of approximation and is thus able to show the existence of a third ‘harmonic’ in the FRF. A comparison is made with previous work where an approximation to the FRF was computed using the Volterra series.

© 2010 Elsevier Ltd. All rights reserved.

### 1. Introduction

Experimental structural dynamics is commonly based on the computation of a number of features of vibration, based on the frequency domain representation of time data. The most often-used feature is arguably the frequency response function (FRF), which gives a directly interpretable representation of the response behaviour of a given structure. Information which is immediately available from the FRF includes the position (in frequency) of resonances and the extent to which the resonances are damped. The FRF is of such importance that standard instrumentation is available for its measurement in the laboratory. Such instrumentation varies considerably in its versatility (and cost), but common to all systems is the fact that computation of the FRF is based on standard Fourier analysis and linear system theory. In many cases, this is perfectly adequate for vibration testing; however, in the case where a significantly nonlinear system is under test, the measured FRFs can display features which are absent in the linear case. Such features can include the presence of FRF peaks at multiples (harmonics) of the fundamental resonance frequencies.

One might argue that the FRF, founded as it is in linear system theory, is not conceptually appropriate for the study of nonlinear systems. This argument is countered by the fact that standard spectrum-based estimates of the FRF, applied unmodified to nonlinear systems, can often expose the nonlinearity and shed light on its nature. A simple approach to the diagnosis of nonlinearity, which is of enormous importance in itself in experimental structural dynamics, is to extract FRFs corresponding to different levels of excitation; any difference between the measured FRFs supports the conclusion that the system is nonlinear. Changes in the FRF peak frequencies or peak widths as the excitation level changes can indicate whether the system is subject to stiffness or damping nonlinearities; in the former case one can see if the stiffness

\* Corresponding author.

E-mail address: [k.worden@sheffield.ac.uk](mailto:k.worden@sheffield.ac.uk) (K. Worden).

is hardening or softening, in the latter, one might distinguish between polynomial damping and friction. The presence of FRF peaks at harmonics or sums and differences of the main resonances can shed light on whether the nonlinearity is an odd or even function. All of this information is very valuable as a precursor to a full system identification and is available in the laboratory from instrumentation based on linear spectral analysis. These issues are discussed in considerable detail in the monograph [1]. Also discussed there is the use of the Hilbert transform, which can be used to diagnose system nonlinearity on the basis of a single FRF measurement at one excitation level. Extensions to the standard linear frequency domain analysis appropriate to nonlinear systems are available, the most popular being that based on the Volterra series and Higher-order FRFs [1]. As one might expect, the Volterra series provides a much richer characterisation of nonlinear system behaviour than any analysis founded in linear spectral theory; however, it is conceptually much more complex and is not generally available in experimental instrumentation.

Having argued that there is a considerable practical advantage to be gained from applying the standard FRF analysis to nonlinear systems; it is clearly desirable to have analytical expressions for the FRFs concerned in order to shed light on how they deviate in their behaviour from that expected for linear systems—this is a difficult problem. A further issue is that random excitation is commonly used, for practical reasons, in order to extract FRFs, and the analysis of nonlinear system response under random excitation is difficult. One approach to the analytical approximation of nonlinear system FRFs under random forcing is to use the Volterra series mentioned above and its associated Higher-order FRFs. This approach has led to analytical approximations of the FRF of a Duffing oscillator [2] and also to some preliminary analysis for a multi-degree-of-freedom system FRF [3]. The appeal of the Volterra approach for the current authors is based on the fact that it leads to a ‘mode-like’ expansion for the FRF which exposes the positions of the poles, and hence resonances, in a manner which makes direct contact with modal expansions derived from test and linear analysis. The Volterra approach is also well-suited to combination with the Hilbert transform [1]. In general, there has been substantial work in the past which has led to various expressions for approximate FRFs (actually Power Spectral Densities) for nonlinear systems [4–17]. Most of these studies provide estimates which are (often far) better than the Volterra approach; however, they do not usually have the modal form which is considered desirable here. For the purposes of the current discussion, the Refs. [7,9,10] are perhaps the most important as they explicitly derive expressions which accommodate the ‘third-harmonic’ resonance in the Duffing oscillator FRF which is the main concern of this paper. Refs. [12,14,15,17] are noteworthy for their consideration of multi-degree-of-freedom systems. In terms of other quantities of interest from structural testing practice, the Volterra approach has also led to an approximate expression for the coherence of a Duffing oscillator [18].

All of the analytical approximations based on the Volterra series were able to give good qualitative agreement with FRFs estimated from numerical simulations; however, in all cases the quantitative agreement was far less impressive. Two main problems arose in the Volterra analysis; the first was the perennial problem associated with the question of convergence of the series—there is very little one can do to estimate how many terms of the series are needed or indeed if the series is likely to converge. The second problem is a practical one, the calculations grow explosively in complexity as the term order increases. In the light of these issues, it is desirable to investigate alternative means of computing nonlinear system FRFs. One promising approach, dating back to the study by Yar and Hammond [19] is based on the Fokker–Planck–Kolmogorov (FPK) equation which has proved powerful in the analysis of nonlinear random vibration [20,21]. The paper [19] gave a method for computing the FRF of a Duffing oscillator under random excitation; and also gave a ‘mode-like’ expansion. However, the calculation was only carried to ‘first-order’ in a sense which will become clear later. To this degree of approximation, the FPK approach was able to reproduce shifts in the resonance frequency as a function of excitation level; in fact, the results were shown to agree with a statistical linearisation approach. What the analysis did not show, was the presence of maxima in the FRF magnitude at multiples of the fundamental resonance. A further, minor, problem with the paper was that it contained a number of typographical errors which could potentially lead to misunderstandings. Although most of the errors were corrected when the methodology was exposed in the later paper [22], this latter paper only considered a cubically nonlinear first-order system rather than the Duffing oscillator. The modest aim of the current paper is to carry the calculation by Yar and Hammond to a higher-order and thus explain qualitative features of the Duffing oscillator FRF which could be seen in the numerical solution presented in [19]; particularly the peaks at ‘harmonics’ of the fundamental resonance.

When the random excitation applied to a system can be idealised as Gaussian white noise, the solution of the corresponding FPK equations is the transition probability density function. This is considered the most complete statistical description of the process, and when expressed as an expansion of the eigenfunctions of the corresponding FPK operators, can be easily manipulated to give the autocovariance and spectral density functions of the system, these can in turn yield the FRF. Unfortunately, exact solutions to the FPK equations can rarely be found for nonlinear systems, instead methods to approximate the solution must be used.

This paper follows the work of Yar and Hammond [19,22] closely, in using a variational approach to approximate the eigenfunctions of the FPK operators of the Duffing oscillator under Gaussian white noise excitation  $n(t)$

$$\ddot{x} + 2c\dot{x} + x + \varepsilon x^3 = n(t) \quad (1)$$

where

$$E[n(t)] = 0, \quad E[n(t)n(t')] = 2D\delta(t-t')$$

Here,  $c$  represents viscous damping,  $D$  is a constant which measures the white noise intensity, and  $\delta$  is the Dirac delta function;  $E[\cdot]$  is the expectation operator. The coefficient  $\varepsilon$  fixes the relative importance of the cubic term to the linear term,

whose coefficient is unity. It is clearly sufficient to consider the parametrisation in Eq. (1) as any Duffing oscillator can be brought into this form by ‘nondimensionalisation’.

In this paper, just as in Yar and Hammond’s paper, a first-order approximation is initially employed, which is sufficient to reproduce the general features of the statistical linearisation estimate, but not accurate enough to indicate any presence of the poles at odd multiples of the primary resonance which are known to occur from simulation and experiment [23]. The work is then extended to a third-order approximation which successfully shows the existence of a further peak or resonance at three times the fundamental resonance (which need not of course be near the natural frequency of the underlying linear system). The paper follows Yar and Hammond [19] in its description of the basic theory, but attempts to correct the typographical errors. It is useful to recap in any case as this theory will then form the basis of the extended calculations.

## 2. The Fokker–Planck–Kolmogorov (FPK) equations

The transition probability density  $p(x, y, t | x_0, y_0, 0)$  for the Duffing oscillator system of equation (1) satisfies the backwards and forwards FPK equations

$$\begin{aligned}\frac{\partial p}{\partial t} &= L(p) \quad (\text{forward}) \\ \frac{\partial p}{\partial t} &= L^*(p) \quad (\text{backward})\end{aligned}\quad (2)$$

with the initial condition:

$$\lim_{t \rightarrow \tau} p(x, y, t | x_\tau, y_\tau, \tau) = \delta(x - x_\tau) \delta(y - y_\tau).$$

In the above,  $L$  and  $L^*$  are adjoint differential operators defined as follows:

$$\begin{aligned}L(p) &= -y \frac{\partial p}{\partial x} + \frac{\partial}{\partial y} (2cy + x + \varepsilon x^3) p + D \frac{\partial^2 p}{\partial y^2} \\ L^*(p) &= y_\tau \frac{\partial p}{\partial x_\tau} - \frac{\partial}{\partial y_\tau} (2cy_\tau + x_\tau + \varepsilon x_\tau^3) p + D \frac{\partial^2 p}{\partial y_\tau^2}\end{aligned}\quad (3)$$

### 2.1. Eigenfunction expansion of the FPK

Following the work of Johnson and Scott [24], the transition probability density function can be expressed as an expansion of the eigenfunctions of the FPK operators  $L$  and  $L^*$  as follows:

$$p(x, y, t | x_0, y_0, 0) = \sum_{i=1}^{\infty} e^{-\lambda_i t} u_i(x, y) u_i^*(x_0, y_0) \quad (4)$$

where

$$L u_i + \lambda_i u_i = 0 \quad (5)$$

$$L^* u_i^* + \lambda_i u_i^* = 0 \quad (6)$$

Since  $L$  and  $L^*$  are adjoint, their corresponding eigenvalues  $\lambda_i$  are the same. This leads to the following biorthogonality relation which will prove useful later:

$$\int \int u_i u_j^* dx dy = \delta_{ij} \quad (7)$$

where  $\delta_{ij}$  is the Kronecker delta which is unity when  $i=j$ , and zero else. In the paper by Johnson and Scott [24], the parameter  $\varepsilon$  is required to be small; this is a necessity of their method which is based on a perturbation series in  $\varepsilon$ . The current work does not exploit the perturbative approach in [24], and therefore does not need to make formal demands on the size of  $\varepsilon$ ; however, as the approach here is based on series approximations, it is required that the influence of the nonlinearity be weak in some sense and this is ensured by small  $\varepsilon$  or low excitation.

### 2.2. The stationary probability density

An important solution to (5) occurs when  $\lambda_0 = 0$ , i.e.  $L(u_0) = 0$ .  $u_0$  or  $p_s$  is called the stationary probability density and can be used to find the lower-order statistical moments of the process, such as the displacement variance  $\sigma_x^2$ . For the Duffing oscillator

$$u_0 = p_s(x, y) = A e^{-(c/D)(y^2 + x^2 + (\varepsilon/2)x^4)} \quad (8)$$

where the normalisation constant  $A$  is given by

$$A^{-1} = \sqrt{\frac{\pi D}{c}} \frac{\Gamma(1/2)}{(c\varepsilon/D)^{1/4} 4e^{(1/4)(c/\varepsilon D)}} U\left(0, \sqrt{\frac{c}{\varepsilon D}}\right)$$

and  $U(a,b)$  is the parabolic cylindrical function [25].

### 2.3. The operator $G$

Once the stationary probability density function has been found, as in the work of Caughey [26], Yar and Hammond [19,22] and Johnson and Scott [24], it is found to be advantageous to consider the operator  $G$  which is related to  $L$  by the following relation:

$$G(w) = \frac{L(p_s(x,y)w)}{p_s} \quad (9)$$

From which  $G$  is found to be,

$$G(w) = -y \frac{\partial w}{\partial x} + (-2cy + x + \varepsilon x^3) \frac{\partial w}{\partial y} + D \frac{\partial^2 w}{\partial y^2} \quad (10)$$

where

$$G(w) + \lambda w = 0 \quad (11)$$

Now, since,

$$G(w) + \lambda w = 0 \Rightarrow \frac{L(p_s w)}{p_s} + \lambda w = 0 \Rightarrow L(p_s w) + \lambda p_s w = 0$$

it follows that if  $w_i(x,y)$  is an eigenfunction of  $G$  then  $w_i(x,y)p_s(x,y)$  is an eigenfunction of  $L$ . It is also clear here that  $G$  may be obtained from  $L^*$  on simply replacing  $y$  by  $-y$ . Therefore, if  $w_i(x,y)$  is an eigenfunction of  $G$ ,  $w_i(x,-y)$  is an eigenfunction of  $L^*$ . Using these two observations Eq. (4) may now be re-expressed as

$$p(x,y,t|x_0,y_0,0) = p_s(x,y) \sum_{i=1}^{\infty} e^{-\lambda_i t} w_i(x,y) w_i(x_0,-y_0) \quad (12)$$

and the relation (7) can be re-expressed as

$$\int_{-\infty}^{\infty} \int_{-\infty}^{\infty} p_s(x,y) w_i(x,y) w_j(x,-y) dx dy = E[w_i(x,y) w_j(x,-y)] = \delta_{ij} \quad (13)$$

### 2.4. Autocovariance and spectral density functions

Expressions for the autocovariance function and spectral density function in terms of the eigenfunctions  $w_i(x,y)$  may now be easily derived.

The autocovariance function,  $\phi_{xx}(\tau)$  is defined as

$$\phi_{xx}(t_1 - t_0) = E[x(t_0)x(t_1)] = E[x_0 x_1]$$

in an obvious notation. In full,

$$\phi_{xx}(t_1 - t_0) = \int_{-\infty}^{\infty} \int_{-\infty}^{\infty} p_j(x_0, y_0, t_0; x_1, y_1, t_1) x_0 x_1 dx_0 dx_1 dy_0 dy_1 \quad (14)$$

where  $p_j(x_0, y_0, t_0; x_1, y_1, t_1)$  is the complete joint probability density function of  $(x_0, y_0)$  and  $(x_1, y_1)$ . When a stationary solution of the FPK exists, the joint probability density function can be related to the transition probability density by

$$p_j(x, y, t; x', y', t') = p(x', y', t' - t | x, y, 0) p_s(x, y) \quad (15)$$

(which is essentially the definition of a conditional probability).

Using this relation, Eq. (14) becomes

$$\phi_{xx}(\tau) = \int_{-\infty}^{\infty} \int_{-\infty}^{\infty} \int_{-\infty}^{\infty} \int_{-\infty}^{\infty} p(x_1, y_1, \tau | x_0, y_0, 0) p_s(x_0, y_0) x_0 x_1 dx_0 dx_1 dy_0 dy_1$$

which, on substituting Eq. (14) and then Eq. (12), eventually yields,

$$\phi_{xx}(\tau) = \sum_{i=1}^{\infty} e^{-\lambda_i \tau} \gamma_i \eta_i \quad (16)$$

where

$$\gamma_i = \int_{-\infty}^{\infty} \int_{-\infty}^{\infty} xw_i(x,y)p_s(x,y) dx dy = E[xw_i(x,y)]$$

$$\eta_i = \int_{-\infty}^{\infty} \int_{-\infty}^{\infty} xw_i(x,-y)p_s(x,y) dx dy = E[xw_i(x,-y)]$$

The spectral density function is obtained by taking the Fourier transform of the autocovariance function and is straightforwardly found to be

$$S_{xx}(\omega) = 2 \sum_{i=1}^{\infty} \gamma_i \eta_i \frac{\lambda_i}{(\lambda_i^2 + \omega^2)} \tag{17}$$

where  $\gamma_i$  and  $\eta_i$  are as defined above. One can then trivially express the FRF (magnitude) as

$$|H(\omega)| = \sqrt{\frac{S_{xx}(\omega)}{2D}} \tag{18}$$

### 3. Approximating the eigenfunctions of the FPK operators

Since the eigenfunctions of the FPK equations for the Duffing system cannot be found exactly, an approximation technique must be used. A variational method based on the Rayleigh–Ritz method is used here as employed by Yar and Hammond [19] and Atkinson [27].

As shown in Refs. [19,27], approximate eigenfunctions  $w^*(x,y)$  of the operator  $G$  can be expressed in the form

$$w^*(x,y) = \sum_{i=1}^N c_i z_i(x,y) \tag{19}$$

where  $\{z_i(x,y), i = 1, \dots, N\}$  is a set of independent trial functions orthonormal with respect to the stationary density  $p_s(x,y)$ , and  $c_i$  are constants to be found. The constant  $N$  is fixed by the degree of approximation required. Now, upon noting that,

$$p_s(x,y) = a e^{-(c/D)y^2} b e^{-(c/D)(x^2 + (\epsilon/2)x^4)} = p_x(x)p_y(y). \tag{20}$$

where  $a$  and  $b$  are appropriate normalisations, one can see immediately that the trial functions will factorise as

$$z(x,y) = \phi_i(x)H_j(y) \tag{21}$$

where the  $\{\phi_i(x)\}$  will be a set of functions orthonormal with respect to  $p_x(x)$ , and the  $\{H_j(y)\}$  will be a set of functions orthonormal with respect to  $p_y(y)$ . The approximation is further simplified by the observation that only eigenfunctions that are odd polynomials in  $x$  and  $y$  will contribute to the autocovariance and spectral density functions [19]. A set of basis functions  $\{z_k\}$  consisting of products of the odd polynomials of  $\{\phi_i(x), H_j(y)\}$  can therefore be used in the place of the full set in the approximation (19).

Once the basis functions  $\{z_k\}$  have been determined, the constants  $c_i$ , along with the approximate eigenvalues for the original eigenvalue problem (11), are found by solving the matrix eigenvalue problem [19,26]

$$(P + \lambda I)C = 0 \tag{22}$$

where the  $ij$ th element of the matrix  $P$  is  $E[G(z_i)z_j]$ . The eigenvalues  $\lambda$  contain the system resonance frequencies and dampings; the eigenvectors  $C$  specify the coefficients in the linear combination (19) and these are all that are needed in order to construct the FRF from Eq. (18).

#### 3.1. Orthonormal trial functions

To construct the required basis functions, the set  $\{\phi_i(x)\}$  of functions orthonormal with respect to  $p_x(x)$ , and the set  $\{H_j(y)\}$  orthonormal with respect to  $p_y(y)$  must first be found. Since  $y$  is normally distributed, the  $\{H_j(y)\}$  take the form of Hermite polynomials. The required orthonormal set is given by

$$\{H_j(y)\} = \frac{h_j(y)}{||h_j||} \tag{23}$$

where

$$\{h_j(y)\} = \left(\frac{D}{2c}\right)^{-j/2} h_j^{[1]}\left(y\left(\frac{D}{2c}\right)^{-1/2}\right)$$

$$||h_j|| = \sqrt{E[h_j^2]}$$

and  $\{h_j^{[1]}(y)\}$  are the standard Hermite polynomials orthogonal with respect to the normal probability distribution with density  $(1/\sqrt{2\pi})e^{-y^2/2}$  [25].

Because  $p_x(x)$  is not Gaussian the construction of  $\{\phi_i(x)\}$  is approached using the Gram–Schmidt method. This method takes a finite set of linearly independent functions  $\{U_n\}$  and generates an orthogonal set  $\{\psi_n\}$  that spans the same subspace. A set of orthonormalised functions  $\{\phi_n\}$  can then be obtained from the orthogonal sequence. Here  $\{U_n\}$  is taken as the set of monomials  $\{U_n\} = \{1, x, x^2, \dots, x^n\}$ .

### 3.2. Second and higher-order moments of $x$ and $y$

The constructed orthonormal functions will involve the displacement variance  $E[x^2]$ , and higher-order moments such as  $E[x^4]$ . While the stationary probability density can be used to find the second-order moments  $E[x^2]$  and  $E[y^2]$ , recursion relations must be used to express any higher-order moments. If one considers  $E[x^m]$  first, one observes that,

$$E[x^m] = \int_{-\infty}^{\infty} \int_{-\infty}^{\infty} x^m p_s(x, y) dx dy = \int_{-\infty}^{\infty} \int_{-\infty}^{\infty} x^m A e^{-(c/D)(y^2 + x^2) + (\varepsilon/2)x^4} dx dy \quad (24)$$

Integrating by parts, one establishes the following recursion relation:

$$E[x^{m-2}] + \varepsilon E[x^m] = \frac{(m-3)DE[x^{m-4}]}{2c} \quad (25)$$

Using this relation one can find all the higher-order moments providing the displacement variance  $E[x^2]$  is known. Directly from the monograph of To [21], one finds the displacement variance to be

$$E[x^2] = \sqrt{\frac{D}{4c\varepsilon}} U\left[1, \sqrt{\frac{c}{D\varepsilon}}\right] U\left[0, \sqrt{\frac{c}{D\varepsilon}}\right]^{-1} \quad (26)$$

where  $U[a, b]$  is again the parabolic cylindrical function.

It remains now to find an expression for  $E[y^2]$ , and the higher-order moments involving  $y$ . As before, one begins with,

$$E[y^m] = \int_{-\infty}^{\infty} \int_{-\infty}^{\infty} y^m p_s(x, y) dx dy = \int_{-\infty}^{\infty} \int_{-\infty}^{\infty} y^m A e^{-(c/D)(y^2 + x^2) + (\varepsilon/2)x^4} dx dy \quad (27)$$

and integrates by parts; the following recursion relation is found:

$$E[y^m] = \frac{(m-1)DE[y^{m-2}]}{2c} \quad (28)$$

Furthermore, it follows trivially from this recurrence that,

$$E[y^2] = \frac{D}{2c}$$

Everything is now in place to use (19) to approximate the eigenfunctions of the system.

### 3.3. First-order approximation, $N=1$

Yar and Hammond [19] used the approximation in (19) with  $N=2$ , which amounts to a first-order approximation in  $x$  and  $y$ . In this case the basis functions are  $z_1(x, y) = \phi_1(x), z_2(x, y) = H_1(y)$ , where

$$\phi_1 = \frac{x}{\|\psi_1\|} \text{ with } \|\psi_1\| = \sqrt{E[x^2]} = \sigma_x$$

$$H_1 = \frac{y}{\|h_1\|} \text{ with } \|h_1\| = \sqrt{E[y^2]} = \sigma_y = \frac{D}{2c}$$

and the matrix  $P$  of Eq. (22) takes the form,

$$P = \begin{bmatrix} E[G(\phi_1)\phi_1] & E[G(\phi_1)H_1] \\ E[G(H_1)\phi_1] & E[G(H_1)H_1] \end{bmatrix} = \begin{bmatrix} 0 & -\sigma_y \\ \sigma_x & -2c \end{bmatrix}$$

which yields eigenvalues completely consistent with a statistical linearisation approach, as observed in [19].

A Maple routine [28] was used at this point to solve the matrix eigenvalue problem for a low level of excitation, where one would expect to observe the FRF of the underlying linear system; the parameters:  $D=0.005$ ,  $c=0.05$  and  $\varepsilon=0.05$  were adopted (the first in order to ensure near-linearity, the second and third in order to make contact with the results obtained in [19]). With these choices, the approximate eigenvalues of the system were found to be

$$-0.05 \pm 1.002i.$$

Looking at the eigenvalues gives a quick and simple validation as to whether the approximation is working, as the imaginary parts of the eigenvalues should represent the resonances of the system. In this case the imaginary parts of

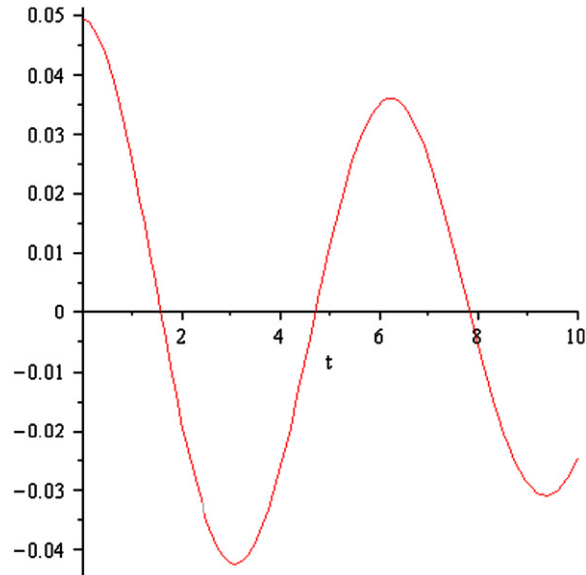


Fig. 1. Autocorrelation function.

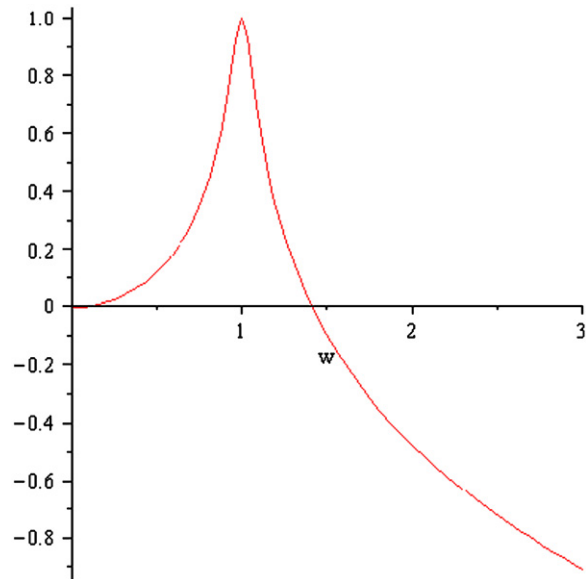


Fig. 2. FRF magnitude.

the eigenvalues are indicating that the primary resonance occurs at around unit frequency, which is expected. The real part of the eigenvalue is simply the damping constant  $c$  which appears directly in Eq. (1).

From this approximation, the autocorrelation function and FRF magnitude were computed using Eqs. (16) and (17), and are shown below. The usual forms associated with the single-degree-of-freedom linear oscillator are observed (Figs. 1 and 2).

In order to provide validation in the case where the forcing actually excites the nonlinearity, it is necessary to use numerical simulation. In this case, the differential equation (1) was stepped forward in time using a standard 4th-order Runge–Kutta scheme as discussed in [29]. In order to have the correct statistics for the forcing, the variance was set at  $\sigma_n^2 = D/\Delta t$ , where  $\Delta t$  is the step-size or sampling interval. In all cases, 9 million samples were generated and an 8192-point FFT was used, with the FRF estimated by averaging the appropriate auto- and cross-spectra. Three FRF estimators are possible [30]:

$$H_1(\omega) = \frac{S_{xy}(\omega)}{S_{xx}(\omega)} \quad (29)$$

$$H_2(\omega) = \frac{S_{yy}(\omega)}{S_{yx}(\omega)} \tag{30}$$

and  $H_v$ —which is the point-wise geometric mean of the first two. It will be seen later that  $H_2$  proves most effective at expressing the nonlinearity; however, first it is useful to validate the numerical algorithms by considering a linear solution with a simple closed-form solution for the FRF,

$$H_l(\omega) = \frac{1}{1-\omega^2 + 2ic\omega} \tag{31}$$

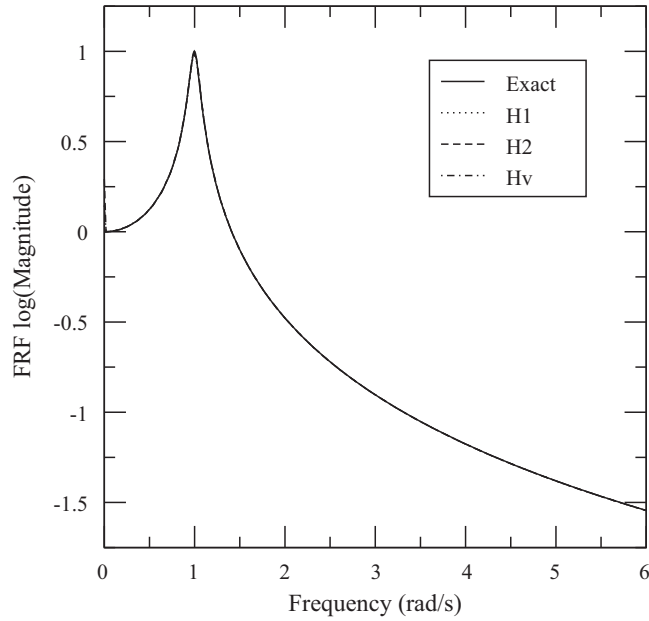


Fig. 3. Magnitude of a linear system FRF: comparison between different FRF estimates from numerically simulated response data and the exact FRF.

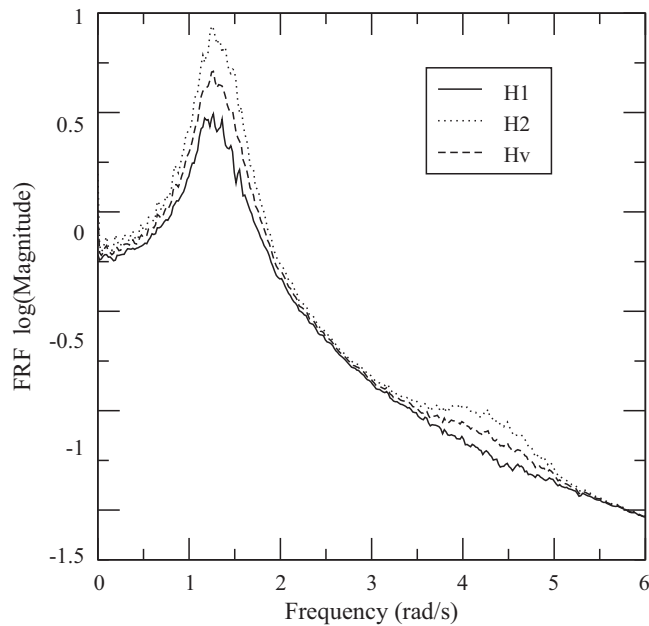


Fig. 4. Magnitude of a nonlinear system FRF: comparison between different FRF estimates from numerically simulated response data.



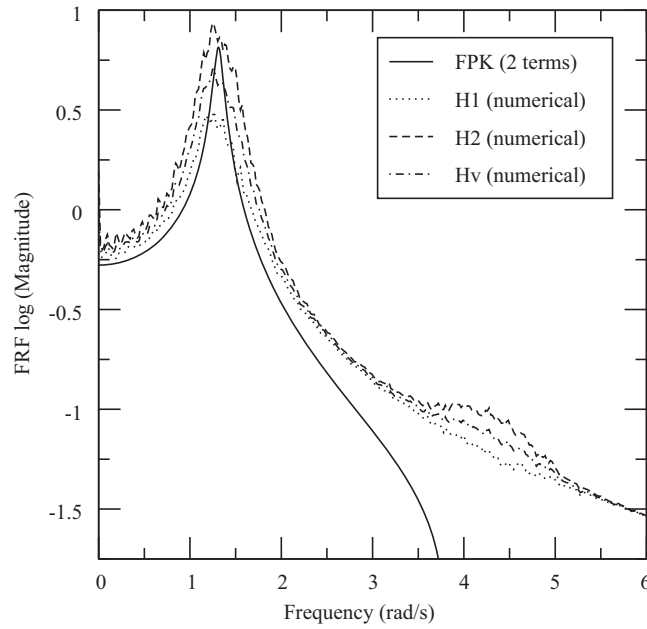


Fig. 5. Magnitude of a nonlinear system FRF: comparison between different FRF estimates from numerically simulated response data and the  $N=2$  FPK estimate.

Taking  $c = 0.05$  and simulating appropriate time data; the numerically estimated FRFs are as shown in Fig. 3 in a comparison with the exact form.

Fig. 3 gives considerable confidence that the numerical results are appropriately accurate. One can now look at the effect of choosing between the different FRF estimators when the system is significantly nonlinear. For the next simulation, the parameters  $D = 1$ ,  $c = 0.05$ ,  $e = 0.05$ , were adopted. The results from different FRF estimators are shown in Fig. 4.

One can immediately observe some of the striking features of a nonlinear system FRF in Fig. 4. In the first case, the fundamental resonance frequency has shifted upwards from the value of 1 rad/s which it would take at low excitation; secondly, there is a clear peak at three times the frequency of the fundamental resonance as discussed in the introduction. One can also see that  $H_2$  shows the latter peak most clearly; this is to be expected as the definition of  $H_2$  depends most on the nonlinear response.

Now, substituting the eigenvalues and eigenvectors obtained in the  $N=2$  FPK analysis above into Eq. (18) gives the analytical approximation to the FRF. (The overall scale of the eigenvectors requires specification at this point, but discussion will be deferred until a more interesting example later.) The computed FRF is shown in Fig. 5 in a comparison with the numerically estimated FRFs.

The results of the comparison in Fig. 5 are interesting. First of all, one observes from Eq. (18) that the FRF estimate from the FPK equation actually corresponds to the  $H_2$  estimate, and this is indeed the closest to the FPK result in terms of peak magnitude. For this reason, only the  $H_2$  estimate will be shown in the following. One can also see that the peak frequency is faithfully reproduced as one might expect from the fact that the  $N=2$  FPK estimate coincides with statistical linearisation. Apart from these points of agreement, the FPK estimate appears to disagree in terms of effective damping (peak width) and thus does not show the spectral broadening expected, as discussed in previous studies [7]. Because comparisons between simulations and the  $N=2$  FPK solution are given in [19], no further results will be shown here, instead the next higher-order of approximation will be explored.

### 3.4. Third-order approximation, $N=6$

Eq. (19) was used with  $N=6$  to compute the third-order approximation of the FPK solution. The required basis functions in this case are  $\{z_1, z_2, z_3, z_4, z_5, z_6\} \propto \{\phi_1(x), H_1(y), \phi_1(x)H_2(y), \phi_2(x)H_1(y), \phi_3(x), H_3(x)\}$ , and  $P$  therefore becomes a  $6 \times 6$  matrix

$$P = \begin{bmatrix} E[G(\phi_1)\phi_1] & E[G(\phi_1)H_1] & E[G(\phi_1)\phi_1H_2] & E[G(\phi_1)\phi_2H_1] & E[G(\phi_1)\phi_3] & E[G(\phi_1)H_3] \\ E[G(H_1)\phi_1] & E[G(H_1)H_1] & E[G(H_1)\phi_1H_2] & E[G(H_1)\phi_2H_1] & E[G(H_1)\phi_3] & E[G(H_1)H_3] \\ E[G(\phi_1H_2)\phi_1] & E[G(\phi_1H_2)H_1] & E[G(\phi_1H_2)\phi_1H_2] & E[G(\phi_1H_2)\phi_2H_1] & E[G(\phi_1H_2)\phi_3] & E[G(\phi_1H_2)H_3] \\ E[G(\phi_2H_1)\phi_1] & E[G(\phi_2H_1)H_1] & E[G(\phi_2H_1)\phi_1H_2] & E[G(\phi_2H_1)\phi_2H_1] & E[G(\phi_2H_1)\phi_3] & E[G(\phi_2H_1)H_3] \\ E[G(\phi_3)\phi_1] & E[G(\phi_3)H_1] & E[G(\phi_3)\phi_1H_2] & E[G(\phi_3)\phi_2H_1] & E[G(\phi_3)\phi_3] & E[G(\phi_3)H_3] \\ E[G(H_3)\phi_1] & E[G(H_3)H_1] & E[G(H_3)\phi_1H_2] & E[G(H_3)\phi_2H_1] & E[G(H_3)\phi_3] & E[G(H_3)H_3] \end{bmatrix}$$

A certain amount of tedious algebra leads to the following expression for  $P$ :

$$\begin{bmatrix}
 0 & -\frac{\sigma_x}{\sigma_y} & 0 & 0 & 0 & 0 & 0 \\
 \frac{\sigma_x}{\sigma_y} & -2c & 0 & 0 & \sqrt{3\varepsilon\sigma_x^2 + 1 - \sigma_y^2/\sigma_x^2} & 0 & 0 \\
 0 & 0 & -4c & 2\sqrt{2\varepsilon\sigma_x\sigma_y}/\sqrt{\sigma_y^2 - \sigma_x^2 - \varepsilon\sigma_x^4} & 0 & -\sqrt{3}\frac{\sigma_y}{\sigma_x} & 0 \\
 0 & 0 & -2\sqrt{2\varepsilon\sigma_x\sigma_y}/\sqrt{\sigma_y^2 - \sigma_x^2 - \varepsilon\sigma_x^4} & -2c & 3\sqrt{3\frac{\sigma_y^2 - \sigma_x^2 - \varepsilon\sigma_x^4}{3\varepsilon\sigma_x^2 + 1 - \sigma_y^2/\sigma_x^2}} & 0 & 0 \\
 0 & -\sqrt{3\varepsilon\sigma_x^2 + 1 - \sigma_y^2/\sigma_x^2} & 0 & -3\sqrt{3\frac{\sigma_y^2 - \sigma_x^2 - \varepsilon\sigma_x^4}{3\varepsilon\sigma_x^2 + 1 - \sigma_y^2/\sigma_x^2}} & 0 & 0 & 0 \\
 0 & 0 & \sqrt{3}\frac{\sigma_y}{\sigma_x} & 0 & 0 & 0 & -6c
 \end{bmatrix}$$

This expression is pleasantly sparse; also the off-diagonal elements hint at some symmetry. Clearly the matrix cannot be antisymmetric as some diagonal elements are non-zero; nonetheless, there is symmetry and it is possible to prove the following result which will be dignified with the title of lemma.

**Lemma.** *With the orthogonal basis assumed above, the matrix  $P$  satisfies:*

$$\begin{aligned}
 P_{ij} &= P_{ji} \text{ if } i-j \text{ is even} \\
 P_{ij} &= -P_{ji} \text{ if } i-j \text{ is odd}
 \end{aligned}$$

**Proof.** One begins with the definition

$$P_{ij} = E[G(w_i)w_j] = \int_{-\infty}^{\infty} p_s(x,y)G(w_i(x,y))w_j(x,y) dx dy$$

The latter expression can be manipulated, based on the definition of  $G$  in Eq. (9),

$$\begin{aligned}
 \int_{-\infty}^{\infty} p_s(x,y)G(w_i(x,y))w_j(x,y) dx dy &= \int_{-\infty}^{\infty} p_s(x,y)[L(p_s(x,y)w_i(x,y))/p_s(x,y)]w_j(x,y) dx dy \\
 &= \int_{-\infty}^{\infty} L(p_s(x,y)w_i(x,y))w_j(x,y) dx dy = \int_{-\infty}^{\infty} p_s(x,y)w_i(x,y)L^*(w_j(x,y)) dx dy
 \end{aligned}$$

according to the definition of the adjoint [19]. Now, one makes the trivial change of variables  $y \rightarrow -y$  and the property that  $L^*(x,y) = G(x,-y)$  to obtain

$$P_{ij} = \int_{-\infty}^{\infty} p_s(x,-y)w_i(x,-y)G(w_j(x,-y)) dx dy$$

Now, for the Duffing oscillator, one has  $p_s(x,y) = p_s(x,-y)$ . Further, with the labelling of the basis functions adopted above, one has

$$\begin{aligned}
 \text{if } i = 1, 3, 5 : w_i(x,y) &= -w_i(x,-y) \\
 \text{if } i = 2, 4, 6 : w_i(x,y) &= w_i(x,-y)
 \end{aligned}$$

and the result follows.  $\square$

This result is very useful. If one can maintain an appropriate ordering of the basis functions for an even higher approximation, one will have the same result; independent of ordering, one will still only have the same independent number of elements of  $P$  as if it were symmetric. In fact, the matrix  $P$  here has all the off-diagonal elements with  $i-j$  even, equal to zero, and this means that  $P$  is the sum of a diagonal and a skew-symmetric matrix.<sup>1</sup> It may be that this is a general result; however, the authors cannot find an immediate reason for this. If this were to be true generally, it would simplify the derivation of  $P$  for higher-order approximations and could potentially simplify the eigenproblem.

A Maple routine was once again used to solve the  $6 \times 6$  matrix eigenvalue problem (22). As before, for a quick validation of the approximation one can once again consider the approximate eigenvalues. For a higher level of excitation which is expected to force some nonlinear behaviour: for  $D=1$ ,  $c=0.05$  and  $\varepsilon=0.001$ , the approximate eigenvalues of the system are found to be

$$\begin{aligned}
 -0.016 + 1.027 i & \quad -0.016 - 1.027 i \\
 -0.070 + 3.081 i & \quad -0.070 - 3.081 i \\
 -0.048 + 1.012 i & \quad -0.048 - 1.012 i
 \end{aligned}$$

As expected, one pair of the eigenvalues have imaginary part close to unity, representing the frequency corresponding to the primary resonance. The second pair have imaginary parts close to three, which confirms that the approximation is

<sup>1</sup> The authors would like to thank one of the anonymous referees for this observation.

recreating the secondary resonance at three times the natural frequency. The third pair of eigenvalues suggest the presence of a double pole at around unit frequency.

The FRF is computed using Eq. (18) as before, once the eigenvalues and eigenvectors of  $P$  are known. The only real subtlety here relates to the normalisation of the eigenvectors. Given an eigenvector  $\{c_1, c_2, c_3, c_4, c_5, c_6\}$ , this is only known up to an overall scale, so an equally good eigenvector would be  $k\{c_1, c_2, c_3, c_4, c_5, c_6\}$  for any real  $k$ . However, the linear combinations in Eq. (19) are required to be orthonormal, in particular  $E[w^*(x, y)w^*(x, -y)] = 1$ . Now the trial functions in the basis are themselves orthonormal and substituting the linear expansion (19) into the orthonormality relation gives, with the ordering of basis functions adopted here,

$$k^2(c_1^2 - c_2^2 + c_3^2 - c_4^2 + c_5^2 - c_6^2) = 1$$

and this fixes the overall scale of the eigenvectors. In the simulations conducted here, in order to make contact with the parameters chosen for the study in [19], a value of unity is taken for  $D$  and the following combinations of  $c$  and  $\varepsilon$  are

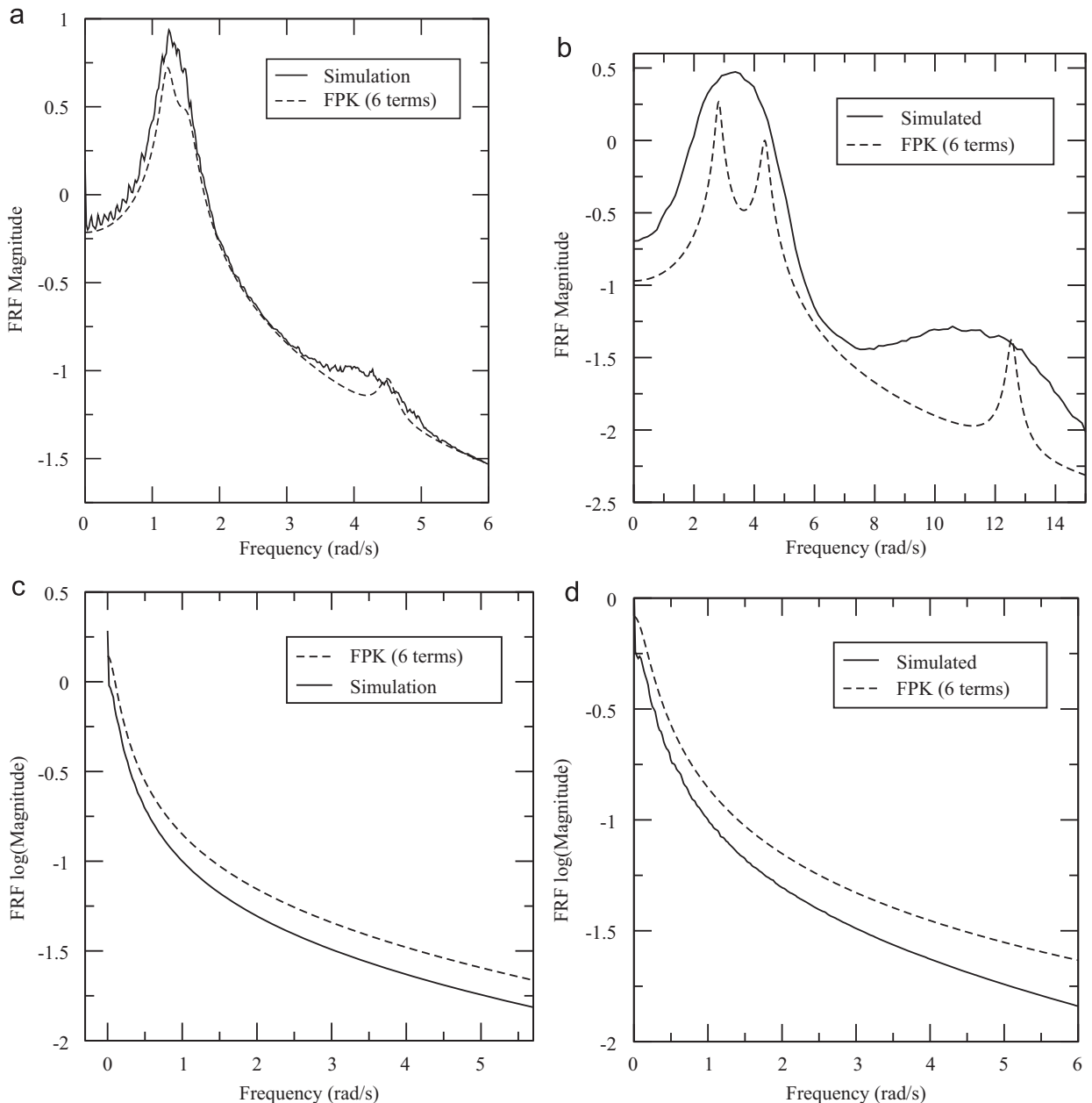


**Fig. 6.** Comparison between FPK analytical approximation to FRF (6 terms) and numerical simulation: (a)  $c = 0.05, \varepsilon = 0.05$ ; (b)  $c = 0.05, \varepsilon = 0.5$ ; (c)  $c = 0.5, \varepsilon = 0.05$ ; and (d).  $c = 0.5, \varepsilon = 0.5$ .

considered:  $\{(0.05, 0.05), (0.05, 0.5), (0.5, 0.05), (0.5, 0.5)\}$ . These are very high values of the parameters concerned and therefore constitute quite a severe test of the expansions. Fig. 6 summarises the results of the computations.

The results are rather interesting (Figs. 6c and d, less so because the very high damping has destroyed the modal nature of the FRF). However, Fig. 6a shows very good agreement with the FRF compared with the result given in Fig. 5 for the  $N=2$  estimate. The approximation now shows the correct level of effective damping (peak width). More importantly, the analytical approximation shows a peak at a frequency three times that of the fundamental resonance as hoped. In Fig. 6b, the level of nonlinearity is very high indeed and the approximation is having difficulty; in order to reproduce the width of the main peak the approximation has produced a split peak; one would anticipate that a better representation would be obtained at the next order of approximation. The next highest approximation would have 12 terms corresponding to six individual peaks with which to construct the FRF; it would be expected that, at that order of approximation, a peak at five times the frequency of the fundamental resonance would appear.

#### 4. Comparison with the Volterra series

In order to make contact with previous work in [2] on the analytical approximation of the FRF, one can compare the current results with those obtained using the Volterra series. To the highest order approximation pursued in [2], one finds

$$A(\omega) = H_I(\omega) - \frac{3D\varepsilon}{2c} H_I(\omega)^2 + \frac{9D^2\varepsilon^2 H_I(\omega)^2}{4c^2} \left( 1 + H_I(\omega) + \frac{2c^2}{\pi^2} I(\omega) \right) \quad (32)$$

where

$$I(\omega) = \frac{-\pi^2(\omega^2 - 3\omega_d^2 - 10i\omega - 27c^2)}{4c^2(\omega - \omega_d - 3ic)(\omega + \omega_d - 3ic)(\omega - 3\omega_d - 3ic)(\omega + 3\omega_d - 3ic)} \quad (33)$$

with  $\omega_d^2 = 1 - c^2$  and  $H_I$  given by Eq. (31). If one evaluates the expression in Eq. (32) for the case:  $c = 0.05$ ,  $\varepsilon = 0.05$ , the result shown in Fig. 7 is obtained (in comparison with the numerically simulated FRF). The results are rather poor; qualitative agreement is largely absent, although there is good agreement in the tail where the effects of nonlinearity are not felt. It is not surprising that the Volterra result is poor here. As indicated above, the value of the cubic stiffness coefficient is very high here and perhaps more importantly, the value of  $D=1$ , is completely inconsistent with regarding  $D$  as a ‘small’ expansion parameter. In defence of the Volterra result, one can at least point out that the peak at three times the fundamental resonance frequency is represented. The poor quantitative approximation provided by Volterra estimates was also highlighted in [13].

The two analytical results are not directly comparable in all respects; however, there at least two points of contact:

1. To the lowest order of approximation, a single pole in the expression represents the modal structure in the FRF. The difference between the two approaches is that the Volterra approach generates the FRF of the underlying linear system and the pole corresponds to its natural frequency. In contrast, the pole in the FPK lowest-order approximation

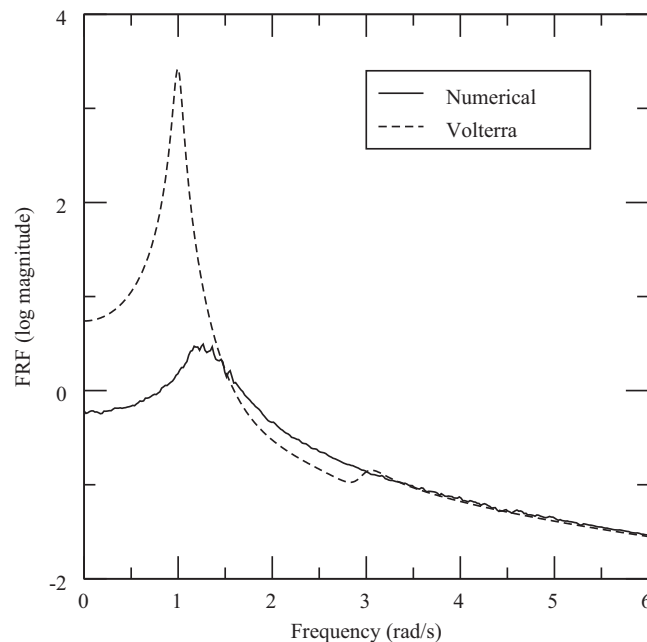


Fig. 7. Comparison between Volterra approximation to FRF and numerical simulation for  $c = 0.05$  and  $\varepsilon = 0.05$ .

corresponds to the statistical linearisation result and can therefore follow changes in excitation level; this makes the FPK approach arguably superior. When the order of approximation is increased, both methods introduce a pole corresponding to the third 'harmonic'. In the case of the Volterra approach, this is at three times the resonance frequency of the underlying nonlinear system; in the case of the FPK equation, the harmonic resonance appears to follow the fundamental resonance under changes in excitation level. Both methods (sort of) increase the multiplicity of the pole at the fundamental resonance in the higher-order approximation. In qualitative terms, the fixed nature of the Volterra poles seems to make it much harder for the FRF approximation to shift the resonance peak when the excitation level increases, this is clear from Fig. 7.

- Both methods place all the poles of the approximate FRF in the lower half of the complex plane. As discussed in [2], this was regarded as a merit of the Volterra approximation as it goes some way to explaining why the Hilbert transform test for nonlinearity gives a null result if applied to an FRF from random excitation. However, it appears that the FPK FRF approximation shares the property and therefore also 'explains' the Hilbert transform result. Because the FPK approximation also gives much better fidelity in modelling the FRF at higher levels of excitation and nonlinearity, it should perhaps be regarded as the superior approach.

In terms of computational effort, both the FPK and Volterra approaches are algebraically demanding. In the case of the Volterra approach, the analyst is faced with the evaluation of many multiple integrals by the calculus of residues. In the case of the FPK equation, one is faced with the problem of populating the  $P$  matrix. On balance, the FPK approach appears to require less effort; a further advantage is that the symmetry relations obeyed by the elements of the  $P$  matrix offer a check as the calculation proceeds.

## 5. Conclusions

The main result of the paper is an extended approximation to the Duffing oscillator FRF which reproduces features of the FRF absent from the lower-order approximation computed previously by Yar and Hammond. The main feature of interest is the appearance of a peak in the FRF at three times the frequency of the fundamental resonance; apart from this, the approximation matches numerically simulated FRFs more closely. The research is part of a general programme of work by the authors on the analytical approximation of various observable quantities typically measured during structural dynamic test. Previous work in this programme was centred on the use of the Volterra series; while this was successful in reproducing the qualitative features of the various observables, quantitative agreement was sometimes absent. The current approach based on the Fokker–Planck–Komogorov equation appears to offer better qualitative fidelity at a lower computational cost. Further research will extend the computations to higher-order, consider different nonlinear systems and extend the approach to multi-degree-of-freedom systems. The FPK approach adopted here appeals to the authors largely because of the 'mode-like' expression it provides; if one is not too concerned with this, it has to be admitted that there are more accurate and less algebraically-demanding approaches to FRF and spectrum estimation, as a consideration of the references here would show.

## Note added in proof

After the article had reached the proof stage, another anonymous review was made available to the authors. This quite rightly pointed-out deficiencies in the citations of previous work. The authors have added a number of appropriate references as a result of this, and would like to thank the reviewer for his or her comment.

## References

- [1] K. Worden, G.R. Tomlinson, *Nonlinearity in Structural Dynamics: Detection, Identification and Modelling*, Institute of Physics Press, 2001.
- [2] K. Worden, G. Manson, Random vibrations of a Duffing oscillator using the Volterra series, *Journal of Sound and Vibration* 217 (4) (1998) 781–789.
- [3] K. Worden, G. Manson, Random vibrations of a multi degree-of-freedom nonlinear system using the Volterra series, *Journal of Sound and Vibration* 226 (1999) 397–405.
- [4] M.I. Dykman, M.A. Krivoglaz, Time correlation functions and spectral distributions of the Duffing oscillator in a random force field, *Physica A* 104 (1980) 495–508.
- [5] M.I. Dykman, S.M. Soskin, M.A. Krivoglaz, Spectral distribution of a nonlinear oscillator performing Brownian motion in a double-well potential, *Physica A* 133 (1985) 53–73.
- [6] M.I. Dykman, R. Mannella, P.V.E. McClintock, F. Moss, S.M. Soskin, Spectral density of fluctuations of a double-well Duffing oscillator driven by white noise, *Physical Review A* 37 (1988) 1303–1313.
- [7] R.N. Iyengar, Higher-order linearization in non-linear random vibration, *International Journal of Non-Linear Mechanics* 23 (1988) 385–391.
- [8] R.N. Miles, An approximate solution for the spectral response of Duffing's oscillator with random input, *Journal of Sound and Vibration* 132 (1989) 43–49.
- [9] V.R. Roy, P.D. Spanos, Power spectral density of nonlinear system response: the recursion method, *Journal of Applied Mechanics* 60 (1993) 358–365.
- [10] R. Bouc, The power spectral density of response for a strongly non-linear random oscillator, *Journal of Sound and Vibration* 175 (1994) 317–331.
- [11] C. Soize, Stochastic linearization method with random parameters for SDOF nonlinear dynamical systems: prediction and identification procedures, *Probabilistic Engineering Mechanics* 10 (1995) 143–152.
- [12] C. Soize, O. Le Fur, Modal identification of weakly non-linear multidimensional dynamical systems using a stochastic linearization method with random coefficients, *Journal of Engineering and Applied Science* 11 (1997) 37–49.
- [13] G.Q. Cai, Y.K. Lin, Response spectral densities of strongly nonlinear systems under random excitation, *Probabilistic Engineering Mechanics* 12 (1997) 41–47.

- [14] S. Bellizzi, R. Bouc, Analysis of multi-degree of freedom strongly non-linear mechanical systems with random input. Part I: non-linear modes and stochastic averaging,, *Probabilistic Engineering Mechanics* 14 (1999) 229–244.
- [15] S. Bellizzi, R. Bouc, Analysis of multi-degree of freedom strongly non-linear mechanical systems with random input. Part II: equivalent linear system with random matrices and power spectral density matrix, *Probabilistic Engineering Mechanics* 14 (1999) 245–256.
- [16] P.D. Spanos, M. Di Paola, G. Failla, A Galerkin approach for power spectrum determination of nonlinear oscillators, *Meccanica* 37 (2002) 51–65.
- [17] G. Failla, P.D. Spanos, M. Di Paola, Response power spectrum of multi-degree-of-freedom nonlinear systems by a Galerkin technique, *Journal of Applied Mechanics* 70 (2003) 708–714.
- [18] K. Worden, G. Manson, A Volterra series approximation to the coherence of the Duffing oscillator, *Journal of Sound and Vibration* 286 (2005) 529–547.
- [19] M. Yar, J.K. Hammond, Spectral analysis of a randomly excited Duffing system, *Proceedings of the 4th International Modal Analysis Conference*, Los Angeles, 1986.
- [20] Y.K. Lin, G.Q. Cai, *Probabilistic Structural Dynamics*, McGraw-Hill Professional, 2004.
- [21] C.W.S. To, *Nonlinear Random Vibration*, Swets & Zeitlinger, 2000.
- [22] M. Yar, J.K. Hammond, Approximate eigenfunction analysis of first order non-linear systems with application to a cubic system, *Journal of Sound and Vibration* 111 (3) (1986) 457–466.
- [23] A.H. Nayfeh, D.T. Mook, *Nonlinear Oscillations*, Wiley, New York, 1995.
- [24] J.P. Johnson, R.A. Scott, Extensions of eigenfunction-expansion solutions of a Fokker–Planck equation—II. second order system, *International Journal of Non-Linear Mechanics* 15 (1980) 41–56.
- [25] A. Erdélyi, W. Magnus, F. Oberhettinger, F.G. Tricomi, *Higher Transcendental Functions Volumes 1 to 3. Based, in part, on Notes Left by Harry Bateman and Compiled by the Staff of the Bateman Manuscript Project*, McGraw-Hill, New York, 1953.
- [26] T.K. Caughey, Nonlinear theory of random vibrations, *Advances in Applied Mechanics* 11 (1963) 209–253.
- [27] J.D. Atkinson, Eigenfunction expansions for randomly excited non-linear systems, *Journal of Sound and Vibration* 30 (2) (1973) 153–172.
- [28] *Maple 12—Software for Algebraic Computing*. Maplesoft Ltd., 2009.
- [29] W.H. Press, S.A. Teukolsky, W.T. Vetterling, B.P. Flannery, *Numerical Recipes 3rd Edition: The Art of Scientific Computing*, Cambridge University Press, 2007.
- [30] D.J. Ewins, *Modal Testing: Theory, Practice and Application - 2nd Edition*, Wiley-Blackwell, 2000.